Nanoscale

PAPER

Cite this: *Nanoscale*, 2019, **11**, 9691

Cold-swappable DNA gels†

Francesca Bomboi,‡[a] Debora Caprara,‡[a] Javier Fernandez-Castanon[a] and Francesco Sciortino*[a,b]

Received 5th February 2019,
Accepted 26th April 2019

DOI: 10.1039/c9nr01156k

rsc.li/nanoscale

We report an experimental investigation of an all-DNA gel composed by tetra-functional DNA nanoparticles acting as network nodes and bi-functional ones acting as links. The DNA binding sequence is designed to generate at room and lower temperatures a persistent long-lived network. Exploiting ideas from DNA-nanotechnology, we implement in the binding base sequences an appropriate exchange reaction which allows links to swap, constantly retaining the total number of network links. The DNA gel is thus able to rearrange its topology at low temperature while preserving its fully-bonded configuration.

Introduction

Nodes and links define, in a very general way, the structural and topological properties of networks. In molecular systems, nodes are provided by particles with well-defined functionality and links by specific interparticle interactions.[1,2] In all-DNA gels, nodes and links can be produced by the spontaneous self-assembly of strands of properly selected base sequences, a powerful method for synthesising nanometric DNA particles[3,4] with precise functionality and binding selectivity.[5–8] The fine control over valence and interaction strength resulting from the selection of appropriate sequences provides a unique tool to direct the assembly of disordered bulk materials with purposely-designed temperature-dependent properties. For example, DNA-made nano-stars with three or four double-stranded arms, terminating with a single-stranded sticky sequence, have been shown to aggregate on cooling, forming networks with prescribed node functionality and, despite their intrinsic disorder, well-controlled real-space structure.[9] The selection of the DNA bases also makes it possible to control the lifetime of the network links, a property which has historically been used to classify molecular networks into chemical and physical gels.[1,2] While in covalently linked (chemical) gels the lifetime of the links is infinite, in the case of physical gels continuous breaking and re-forming of bonds generates a dynamic evolution of the network topology, which gives rise to intrinsic restructuring capabilities that can be exploited in a large variety of applications.[10] Usually, chemical gels are stable and able to sustain large strains but their structure is irreversibly encoded in their aggregation process, hindering the ability to release unwanted stresses. Physical gels restructure themselves but their mechanical stability is affected by the finite lifetime of their interparticle bonds. A recently introduced novel class of polymeric networks, named vitrimers,[11–13] lays in the middle between chemical and physical gels. In vitrimers the number of links in the system is constantly preserved as in chemical gels but the network topology (*i.e.* the local connection between the nodes) evolves in time as in physical gels, resulting in materials which inherit the qualities of both original classes. Vitrimers exploit the strength of the covalent bonds but at the same time incorporate the ability to restructure the network topology and release any frozen stress by suitably catalysed swap reactions which are able to exchange existing links without altering their total number.[11,12]

In DNA nanotechnology,[3] strand displacement reactions have been proposed as a highly versatile and programmable tool to dynamically reconfigure pre-hybridised DNA strands.[14–17] The displacement is thermodynamically driven forward by the binding of the invading strand to the toehold, a short single-stranded sequence localised next to the target strand which provides the attachment point to start the reaction. After binding to the toehold, a random walk of the branch point (branch migration) brings to a progressive replacement of the incumbent bases. The kinetics of the strand displacement can be regulated by varying the sequence and length of the toehold or by inserting mismatched basepairs[18–20] and inert spacers[21] which act as kinetic barriers. Applications range from the implementation of DNA-based molecular motors[22] and logic circuits[23] to the programmable assembly of DNA-nanoparticles,[24,25] of emulsion droplets[17,26] and of proteins.[27] The toehold strand displacement reaction can be transformed in an exchange reaction (indicating that the product state includes a novel toehold which can initiate the back reaction) with a careful design of the DNA sequence.[14,28]

[a]*Physics Department, Sapienza University, P.le Aldo Moro 5, 00185 Rome, Italy. E-mail: Francesco.sciortino@uniroma1.it*
[b]*CNR-ISC c/o Sapienza, P.le Aldo Moro 5, 00185 Rome, Italy*

†Electronic supplementary information (ESI) available. See DOI: 10.1039/C9NR01156K

‡These authors contributed equally to this work.

The ability to control the structure and the node functionality of such DNA-based network and the possibility to incorporate in the interparticle bond the design of an appropriate exchange reaction is here exploited to experimentally realise an all-DNA gel capable of switching the network links, although at ambient T the link strength is hundred times the thermal energy k_BT. Borrowing from the vitrimer idea,[11] we realise a binary mixture of DNA nano-stars with non-stoichiometric composition. Specifically, we mix N_A tetra-functional (A) and N_B bi-functional (B) DNA nanoparticles (Fig. 1(a and b)) that can selectively form only AB bonds. By controlling the composition $x \equiv N_A(N_A + N_B)$ we precisely control the structure of the network and the number of network defects. Indeed, if $N_B = 2N_A$ (corresponding to $x = 0.\bar{3}$) the fully-bonded network is composed by tetra-functional nodes (the tetra-functional particles) all connected by links (the bi-functional particles), a topology similar to the one observed in network forming liquids as water (H_2O) or silica (SiO_2). If $x < 0.\bar{3}$, even when all tetramers are bonded, there is a finite fraction of B particles which remains unbonded, generating dangling network links or isolated unbonded B particles (see Fig. 1(c)). Hereon, we will refer to these unbonded binding sites as the network defects. By appropriately selecting the binding base sequence, we implement in the tips of the A and B particles an exchange toehold-mediated mechanism.[28] This reaction is activated by the presence of a B-particle with an unbonded end in the proximity of an existing link. The binding of the B particle to the complementary toehold located on the link initiates the exchange reaction which can conclude itself by the detachment of the incoming strand (leaving the network topology unchanged) or by the detachment of the displaced strand (resulting into a local modification of the network topology). Fig. 1(d–g) shows a cartoon of a swap event.

To the best of our knowledge, it is the first time that a bond-swapping process, which can be initiated by both sides of the bond, is encoded in a network entirely made of mutually binding DNA nanoparticles, in which both incumbent and displaced strands are not diffusing units but belong to the gel structure. This intrinsic dynamic behaviour, which occurs *via* toehold-exchange reactions, confers to the system restructuring properties with promising applications in nanomedicine and biotechnological fields.[29–31]

In this study we select tetra-functional (A) DNA nanoparticles to generate a network of tetra-functional nodes. The flexibility in the DNA design would also allows us, in principle, to use particles with a different number of arms, as shown in previous studies of DNA gels. The functionality of the nodes controls the region of the thermodynamic stability of the gel[6] as well as the gel mechanical properties[32] and can thus be exploited for a detailed design of the material properties (see ESI† for further discussion on the role of the particle functionality).

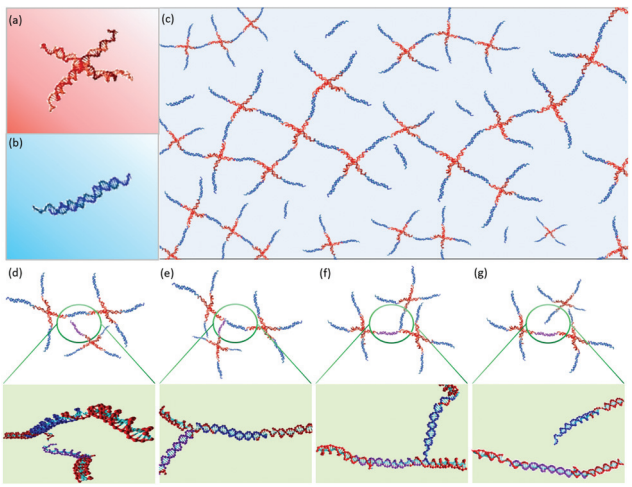

Fig. 1 Representation of a tetra-functional A (a) and a bi-functional B (b) DNA nanoparticle. (c) Schematic representation of the binary gel, composed by tetra-functional A nano-stars connected *via* B dimers. The excess concentration of dimers guarantees that all nano-stars are bonded at low T. The composition is chosen in such a way that a percolating network of nano-stars is present. (d–g) Snapshots of the swapping process. (d) Shows the DNA strands composing the link connecting to nodes (star-arm/dimer/star-arm, coded as red-blue-red) and an incoming free end departing from a close by node (red-violet). (e) Shows the incoming free end attached to the toehold. (f) Shows the complex after the swap process, with the original dimer still attached to the opposite toehold. (g) The completely swapped configuration, in which now the node-node connection is provided by the violet strands.

Methods

System design

Tetra-functional DNA nano-stars, previously used as building blocks for equilibrium DNA hydrogels[9,33,34] are used as A particles. These nano-sized star-shaped DNA structures are composed by four double-stranded arms of 25 basepairs with a flexible core of four unpaired adenines which provide structural flexibility[35] and self-assemble at $T > 80$ °C (see ESI†). Each arm of the nano-star terminates with a single-stranded sequence of 15 bases (P sequence) (Fig. 2(a)). Instead, B dimers are composed by a double-stranded segment of 25 basepairs terminating, on the two opposite sides, with two different single-stranded overhangs E1, E2 (Fig. 2(b)).

Two system cases are specifically investigated in this work. In the first case (named swapping sample), E1, E2 share a similar sequence of 7 bases and differ in the remaining 4 bases. The selected base sequences allow only P–E1 or P–E2 bonds, both forming 11 basepairs (Fig. 2(c)). The remaining unpaired 4 bases of the P sequence act as a toehold for the swapping process. In the second case (named non-swapping sample), the DNA sequences are identical to the one of the swapping sample except for the four toehold bases in the P sequence which have now been removed (shortening the sequence to 11 bases). The DNA sequences defining the A and B particles are shown in Fig. 2 and properly listed (both for the swapping and the non-swapping case) in the ESI.†

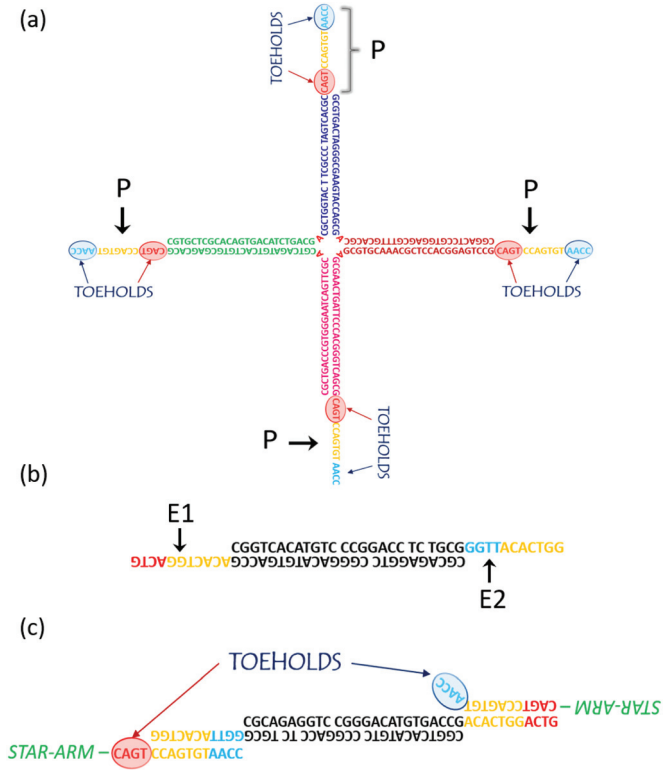

Fig. 2 (a) Sequence design of a tetra-functional A particle, consisting of four arms each terminating with an identical P sticky end. The P sequence includes two different regions of 4 bases each which will act as toeholds. (b) Sequence representation of a bi-functional B nanoparticle, made of a double-stranded region (black) and terminating with two different single-stranded overhangs, E1 and E2. (c) Schematic representation of the bindings between A and B particles: the P sticky sequence can bind with E1 or E2 leaving two unpaired toeholds.

The difference between the length of the double-stranded sections of the nano-structures (25 basepairs for each A particle arm) and the length of the P–E1 or P–E2 hybridised segments (11 basepairs) ensures that there is a well-defined T-gap between the T at which nano-structures self-assemble (T_{ns}) and the T at which they start to bind T_{net}. At very high T, *i.e.* for $T > T_{ns}$, the system is a solution of freely-diffusing DNA single strands. By slowly lowering T, complementary strands start to self-assemble so that, for $T_{net} < T < T_{ns}$, the system consists of weakly-interacting A and B nanoparticles. On further cooling ($T < T_{ns}$) A and B progressively bind *via* P–E1 and P–E2 bonds until all possible A–B bonds are formed. At low T, at the stoichiometric concentration $[N_B] = 2[N_A]$ ($x = 0.33$) all B particles will act as links connecting the tetra-functional A nodes. At non-stoichiometric concentrations, in excess of B particles some of the B will have one or both arm tips unbonded, while all the A particles' arm will be bonded to a B arm. If the excess of B particle is limited, the system will retain its ability to form a spanning network. As a guide, it needs to be noted that according to the mean-field theory developed by Stockmayer[36] (reviewed in the ESI†), an infinite cluster (a gel) is present for $0.14 < x < 0.33$, where $x = 0.14$ coincides with the percolation threshold.

Sample preparation

DNA sequences were purchased from Integrated DNA Technologies (IDT) with PAGE purification. Lyophilised samples were reconstituted in a filtered 0.4 M NaCl solution. Particles A and B are pre-assembled by mixing equimolar quantities of the single-stranded components (4 for A and 2 for B), then heating up the mixtures to 95 °C, incubating for 20 minutes and slowly cooling them down to 60 °C with a rate of 15 degrees per hour. The samples are then left to equilibrate for 3 hours at 60 °C. After this step, the samples are brought to room temperature overnight. The annealing is carried out on a Memmert oven.

Hydrogel samples are prepared by mixing A and B particles in specific ratios in order to obtain the following compositions: $x = 0.33$, $x = 0.28$ and $x = 0.25$. Such values have been selected on the basis of the Flory and Stockmayer polymerisation theory. Indeed, the topological properties of this binary network can be evaluated quite accurately in mean-field following the theory of Flory and Stockmayer[36,37] as discussed in the ESI.†

In all samples, the final concentration of the A particles is kept constant and equal to 75 μM, while the concentrations of B particles are 150 μM, 193 μM and 225 μM for the samples at $x = 0.33$, $x = 0.28$ and $x = 0.25$ respectively. After mixing the two components, samples are heated up to 70 °C to facilitate homogenisation.

Dynamic light scattering (DLS)

To prepare for DLS, 40 μl of each sample are loaded into borosilicate glass capillaries (Hilgenberg, inner diameter 2.4 mm). The capillaries and the samples are pre-heated to 60 °C to facilitate loading. All samples are covered by 20 μl of silicon oil and flame sealed to avoid evaporation. Measurements are carried out with a 633 nm Newport Coorporation He–Ne Laser (17 mW) and a Brookhaven Inst. correlator. Samples are immersed in a water bath connected to a thermostat. For each T, we thermalise the sample for 40 minutes before starting measurements lasting at least 10 minutes. Some test measurements have been extended to two hours with no appreciable change.

The correlator provides the autocorrelation functions of the scattered intensity g_2 which are then converted into the autocorrelation functions of the scattered fields g_1 through the Siegert relation. For all the investigated T (20 °C ≤ T ≤ 65 °C), the resulting g_1 curves are fitted to the function:

$$g_1 = C_f e^{-\left(\frac{t}{\tau_f}\right)^{\beta_f}} + C_s e^{-\left(\frac{t}{\tau_s}\right)^{\beta_s}}, \quad (1)$$

where C_f (C_s), τ_f (τ_s), β_f (β_s) are the amplitude, the relaxation time and the stretched exponential factor for the fast (slow) relaxation process, with $C_f + C_s = 1$.

Viscosity

The DLS instrumentation is also used to perform viscosity measurements. Information about the bulk viscosities of the DNA hydrogels is extracted by measuring the Brownian fluctu-

ations of polystyrene (PS) colloids of diameter σ = 530 nm coated with Polyethylene Oxide[38] with a total molecular weight of 10 300 (PS: 3800, and PEO: 6500). The initial concentration of the batch is 10 wt%. Subsequently, it is diluted to obtain the desired final volume fraction of $\varphi = 3.7 \times 10^{-4}$. This value is high enough to ensure that the scattering is exclusively coming from the diffusion motion of colloids, *i.e.*, the DNA hydrogels contribution to the scattering signal is less than 1%. At the same time, this small φ values ensures that colloid–colloid interactions are negligible, as demonstrated in ref. 39. Thus, we can safely assume that the fluctuations in the scattered intensity originate from the brownian motion of the probe colloids.[40] The measured mono-modal scattering is characterised by an exponential autocorrelation function $g_1(t)$ (see ESI†) whose characteristic decay time is $1/Dq^2$, where D is the colloid diffusion coefficient.[40] The sample viscosity η is evaluated as $\eta = \frac{k_B T}{3\pi\sigma D}$, where k_B is the Boltzmann constant.

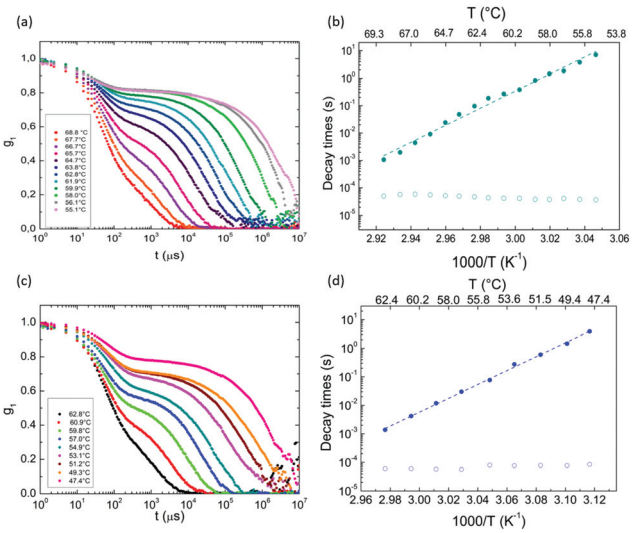

Fig. 3 Dynamics in the non-swapping system induced by T-controlled bond-breaking processes. (a) and (c) show the autocorrelation functions $g_1(t)$ of the scattered light for different T at x = 0.33. In (a) the toehold is inactivated by a proper modification of the base sequence (see Methods). In (c) the absence of swap processes arises from the exact stoichiometry of the sample. Indeed when x = 0.33 all dimer ends are bonded to nano-star arms, resulting in a network with no defects. (b) and (d) show the T dependence of the fast τ_f (empty dots) and slow τ_s (full dots) decay times resulting from a double-stretched exponential fit to $g_1(t)$ (eqn (1)), as discussed in Methods. The dashed line is the best fitting curve of τ_s according to the Arrhenius law, with an enthalpy component of roughly 140 and 111 kcal mol^{-1} respectively. The fast decay times remain rather insensitive of the T in all the investigated T-range.

Results

Non-swapping samples

We start by investigating the properties of the system in the absence of exchange reaction, to quantify the characteristic time scale of the relaxation of the network when the swapping mechanism is missing. Two different cases are investigated: (i) the "non-swapping" system in which, by design, the toehold sequence is not present and thus the swap mechanism can not take place; (ii) the "swapping system" where the toehold is included in the binding sequences, but in which the relative composition of A and B particles is fixed at x = 0.33. At this stoichiometric composition, when all bonds are formed, no network defects are available to start the exchange reaction. In these two cases, the only mechanism for network rearrangement is provided by thermal driven bond-breaking.

Fig. 3(a) shows $g_1(t)$ for different T when no-toeholds ("non-swapping" system) are present. Consistent with previous finding for tetra-functional DNA gels,[34] the correlation function develops a secondary relaxation characterised by a plateau and a slow decay time τ_s, both increasing on cooling. Such relaxation indicates the presence of a network which decorrelates due to bond-breaking and re-forming processes on the time scale τ_s.[6–8,35] The T window where the gel formation is observed (55 °C < T < 70 °C) coincides with the theoretically expected T range (see ESI†) where the 11-base long binding sequence hybridises. The slow time τ_s shows an Arrhenius behaviour as a function of T (Fig. 3(b)) with a slope comparable to the binding sequence hybridisation enthalpy. Previous studies have shown that the characteristic time of the slow relaxation is proportional to the bulk viscosity of the systems.[8,34,39] Thus, data in Fig. 3(a) document the continuous evolution, over four order of magnitude, from a low viscous fluid to a highly viscous gel as T is decreased.

Around 55 °C the density fluctuations decorrelate on a time scale longer than ten-seconds, the longest experimentally accessible value. Similar behaviour is also displayed by the "swapping" system at x = 0.33 (Fig. 3(c and d)). Despite the presence of toeholds in the P binding sequence, the absence of unbonded B ends makes it impossible to initiate any swap process. Even in this system, the dynamics of the gels, measured by the slow relaxation time, is controlled by an Arrhenius decay, always with an activation enthalpy dictated by the 11-base binding sequence. As for the no-toehold system, the onset of the gel is observed in the same T window as the "non-swapping" case. For both systems, extrapolating the Arrhenius dependence of τ_s at room T, the predicted τ_s value is about 10^5 s, consistent with the theoretical estimate of 120 $k_B T$[41] for the free-energy of the eleven binding bases. Thus, at ambient T, both gels retain their network topology for more than a day, effectively behaving as "chemical" gels.

To complete, Fig. 3(b and d) also show the T independence of the fast process, previously interpreted as the network motion on a timescale shorter than the bond-breaking process.[6,34]

Swapping samples

Following, we discuss the dynamics in the presence of exchange processes. We study samples containing the toehold in the binding sequence, but at non-stoichiometric concentrations. Guided by the Stockmayer predictions,[36] we select x = 0.28 and x = 0.25, corresponding respectively to a fraction of

bonded B arm tips equal to ≈0.78 and ≈0.67 or equivalently a fraction of B arm tips available to initiate exchange equal to ≈0.22 and ≈0.33.

These values of x are significantly larger than $x = 0.14$, the value at which a spanning cluster of A particles connected by B links ceases to exist. For the two selected x values 90% of the total particles (A + B) or more belong to the infinite cluster[36] (96% and 90% respectively). In addition, as shown in the ESI,† the majority of the B particles (95% and 89% respectively) are part of the infinite cluster and their swap events effectively contribute to restructure the gel topology. Fig. 4 compares the measured correlation functions for different x values at three selected T. While at high T (Fig. 4(b)) all correlation functions decay on the same timescale, at $T = 57$ °C (Fig. 4(c)), significant differences (about two orders of magnitude in τ_s) appear between the non-swapping ($x = 0.33$) and the two swapping cases ($x = 0.28$ and $x = 0.25$), suggesting that indeed bond reshuffling takes place in the presence of free bridges, altering the local connectivity of the network, ultimately resulting in a decorrelation of the density fluctuations. In addition, the effectiveness of the swapping process demonstrates that the diffusive motion of the network at fixed bonding pattern suffices to bring dangling ends close by existing bonds. Indeed, in the ESI,† we show that the efficiency improves by increasing the local density, *i.e.* by decreasing the average distance between dangling ends and existing bonds. At $T = 34$ °C (Fig. 4(d)), the non-swapping case is not measurable, while the two others have still a decorrelation time smaller than 10 s. To quantify the exchange process more precisely, we compare τ_s for different x samples as a function of the inverse T in Fig. 4(a). At high T, τ_s for all x exhibits an Arrhenius growth with a similar slope dictated by the hybridisation free-energy of the 11 basepairs. In this T region, bond-breaking is still more effective than bond exchange and all samples behave similarly. On lowering T, the presence of the exchange process manifests itself: only samples where the network can reshuffle, due to the presence of unbonded B, decorrelate the local structure. While we are not able to precisely quantify the dependence of τ_s on the concentration of unbonded B, data indisputably demonstrate that the presence of a larger fraction of defects speeds up the network restructuring process. We also note that the T-dependence of τ_s both for the $x = 0.28$ and $x = 0.25$ samples is, at low T, again described by an Arrhenius dependence, this time with an activation energy significantly smaller (approximatively 4/11, see Fig. 4(a)) than the one requested to break the 11-base bond. The 4/11 ratio agrees with the expectation for the T dependence of the implemented exchange reaction. Indeed, the swap reaction is composed by three parts:[14,15,28,42] (i) the attachment of a free B tip to its four-base toehold. In this part, the typical time is controlled by the diffusion of the free tips in space and by their number. (ii) The random walk in the seven-base sequence which concludes in returning to the origin or proceeding to the other end of the sequence. (iii) The evaporation of the incoming or of the incumbent strand. While the random walk part of the process takes place on a flat free-energy landscape[28] and hence its characteristic time is essentially T independent, the detachment rate (part iii) is controlled by the enthalpy of hybridisation of the four toehold bases.[14] It is this four-base enthalpy that controls the T-dependence of the exchange rate, in agreement with our findings.

We finally note that previous works have shown that the relaxation time measured by DLS strongly correlates in DNA-gels with the sample viscosity η,[34,39] as measured by evaluating the diffusion coefficient of a probe colloidal particle or *via* diffusion wave spectroscopy.[43] To provide evidence that, even when swapping events are controlling the network dynamics, η and τ_s are expression of the same relaxation mechanism, we show in Fig. 5 a comparison between the viscosity estimated *via* passive microrheology techniques (see ESI† for further details) with the DLS results for $x = 0.25$. The T dependence of

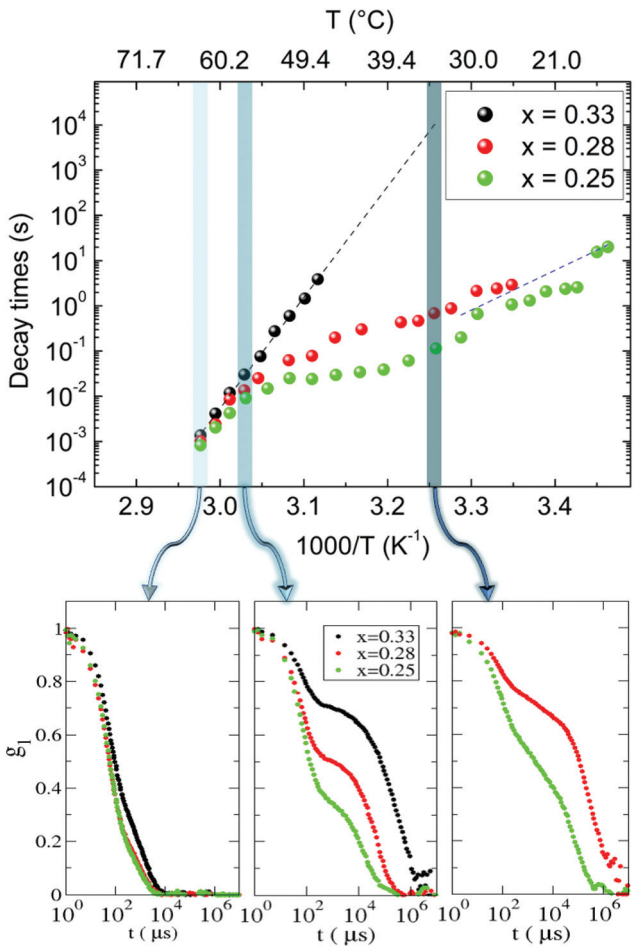

Fig. 4 T dependence of the slow decay times for samples at 3 different system compositions: $x = 0.33$ (black), $x = 0.28$ (red) and $x = 0.25$ (green). The black dashed line is the best-fit with a linear function. The blue line has a slope reduced by 4/11 (4 basepairs of the toeholds to the 11 basepairs of the P–E bonds) with respect to the black one. At the bottom of the figure are reported the correlation functions of the three investigated samples at three different T to show how the different compositions affect the dynamic behaviour of the system. At the lowest T, the sample at $x = 0.33$ relaxes on a timescale much longer than the experimentally measurable time (10 s) and it is thus not reported.

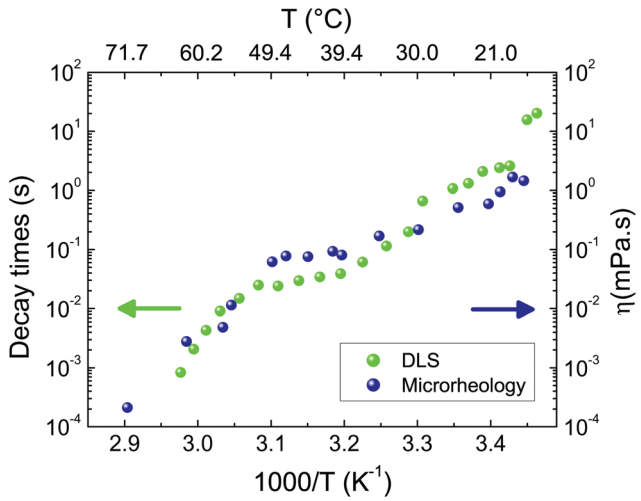

Fig. 5 Comparison between the viscosity measured *via* passive microrheology and the slow relaxation time measured by DLS for the sample at $x = 0.25$.

η tracks the one of τ_s. Such equivalence confirms that the diffusion of the probe particle requires network rearrangements controlled by the swap process. The network restructuring process, mediated by the swapping bonds, is thus at the heart of both the decorrelation of the long wavelength density fluctuations as well as of the bulk viscosity.

Conclusions

We have shown that bringing together the physics of vitrimers and the possibilities offered by DNA-nanotechnology, and in particular by the toehold-mediated strand exchanges, it is possible to realise an all-DNA gel with well defined tetra-functional topology in which, at ambient and lower T, bonds essentially never thermally break but constantly restructure themselves *via* an exchange reaction kinetics. In this system both the strength of the bond and the exchange bond swapping mechanism (in which the successful swap leaves a novel toehold which can initiate the back reaction) are encoded in the design of the DNA sequences.[28] The exhibited dynamic behaviour which ensures self-restructuring and stress-releasing properties[11] jointly with the biocompatibility and non-toxicity of DNA nanoparticles, make the implemented system suitable for *in vivo* engineering applications[29] and for the realisation of smartly-designed functional materials whose mechanical properties can be easily tuned by a precise control over few external parameters. The experimental results, based on Dynamic Light Scattering (DLS) and bulk viscosity, provide evidence of the efficiency of the swap mechanism and of the possibility to control it by simply changing the relative concentration of tetra-functional and bi-functional particles. At room temperature, the speed up in the network restructuring, introduced by the swap mechanism, can be estimated on the basis of the measured Arrhenius dependence of the slow relaxation time in more than five order of magnitude. Finally, we provide experimental evidence that the timescale of the swap dynamics in this system is controlled, at low T, by the toehold evaporation time, a timescale essentially controlled by the length (in number of bases) of the toehold.

In the last years, DNA-made gels have experimented an increasing interest and several nanotechnological applications have resulted. Falling into the class of soft materials, these systems show peculiar mechanical properties that can be easily tuned by varying external parameters. The biocompatibility and non-toxicity make them suitable for cell transplantation and encapsulation[29] as well as for the production of specific proteins.[30] They are biodegradable and can be used to specifically control the release of specific drugs.[29] DNA hydrogels can be characterised by irreversible interactions, in which specific enzymes freeze the system into the desired gel state (allowing to work at physiological conditions), or otherwise can be defined by reversible interparticle bonds in which the bond breaking and re-forming can be thermally controlled.

The restructuring properties of our network gel confer to the system unique mechanical properties, malleability and insolubility, making it a promising biocompatible thermoplastic material for several nanotechnological applications. In addition, the equilibrium-gel nature of this material suggests the absence of spatial heterogeneities and hence that the swap-dynamics is equally active over the entire sample.

Finally we observe that the sample viscosity in the gel phase is essentially controlled by the concentration of network defects. We have demonstrated that it can be varied by over five order of magnitude by design. Thus, for example, these engineered DNA gels could become an ideal material for controlling the release-rate of drugs incorporated in such biocompatible gel. The presented DNA gel, which is able to swap in cold conditions, constitutes a system in which, despite the underlaying network is formed by extremely long living bonds, relaxation of stresses, fracture self-healing and diffusion of guest particles can be tuned at will by the exchange reaction design.

Conflicts of interest

There are no conflicts to declare.

Acknowledgements

We acknowledge support from Regione Lazio (Grant No. 85857-0051-0085). F. S. and J. F. C. acknowledge also support from ETN-COLLDENSE (H2020-MCSA-ITN-2014, Grant No. 642774). We thank D. Pine and Suk Oh for providing us PS colloids coated with PEO, and F. Romano, R. Brady and L. Di Michele for fruitful comments and discussions.

References

1 M. Rubinstein and R. H. Colby, *Polymer Physics*, Oxford University Press, New York, 2003, vol. 23, pp. 1–440.

2 F. Tanaka, *Polymer Physics: Applications to Molecular Association and Thermoreversible Gelation*, Cambridge University Press, 2011, pp. 1–387.
3 N. C. Seeman, *DNA Nanotechnology: From the Pub to Information-Based Chemistry*, Springer, 2018, pp. 1–9.
4 C. Jochum, N. Adžić, E. Stiakakis, T. L. Derrien, D. Luo, G. Kahl and C. N. Likos, *Nanoscale*, 2019, **11**, 1604–1617.
5 Y. H. Roh, R. C. H. Ruiz, S. Peng, J. B. Lee and D. Luo, *Chem. Soc. Rev.*, 2011, **40**, 5730–5744.
6 S. Biffi, R. Cerbino, F. Bomboi, E. M. Paraboschi, R. Asselta, F. Sciortino and T. Bellini, *Proc. Natl. Acad. Sci. U. S. A.*, 2013, **110**, 15633–15637.
7 F. Bomboi, F. Romano, M. Leo, J. Fernandez-Castanon, R. Cerbino, T. Bellini, F. Bordi, P. Filetici and F. Sciortino, *Nat. Commun.*, 2016, **7**, 13191.
8 B.-j. Jeon, D. T. Nguyen, G. R. Abraham, N. Conrad, D. K. Fygenson and O. A. Saleh, *Soft Matter*, 2018, **14**, 7009–7015.
9 J. Fernandez-Castanon, F. Bomboi, L. Rovigatti, M. Zanatta, A. Paciaroni, L. Comez, L. Porcar, C. J. Jafta, G. C. Fadda, T. Bellini and F. Sciortino, *J. Chem. Phys.*, 2016, **145**, 084910.
10 P. Cordier, F. Tournilhac, C. Soulié-Ziakovic and L. Leibler, *Nature*, 2008, **451**, 977.
11 D. Montarnal, M. Capelot, F. Tournilhac and L. Leibler, *Science*, 2011, **334**, 965–968.
12 M. Capelot, M. M. Unterlass, F. Tournilhac and L. Leibler, *ACS Macro Lett.*, 2012, **1**, 789–792.
13 W. Denissen, J. M. Winne and F. E. Du Prez, *Chem. Sci.*, 2016, **7**, 30–38.
14 D. Y. Zhang and E. Winfree, *J. Am. Chem. Soc.*, 2009, **131**, 17303–17314.
15 N. Srinivas, T. E. Ouldridge, P. Šulc, J. M. Schaeffer, B. Yurke, A. A. Louis, J. P. Doye and E. Winfree, *Nucleic Acids Res.*, 2013, **41**, 10641–10658.
16 L. Qian and E. Winfree, *Science*, 2011, **332**, 1196–1201.
17 L. Parolini, J. Kotar, L. Di Michele and B. M. Mognetti, *ACS Nano*, 2016, **10**, 2392–2398.
18 D. Y. Zhang, S. X. Chen and P. Yin, *Nat. Chem.*, 2012, **4**, 208–214.
19 Y. S. Jiang, S. Bhadra, B. Li and A. D. Ellington, *Angew. Chem.*, 2014, **126**, 1876–1879.
20 R. R. Machinek, T. E. Ouldridge, N. E. Haley, J. Bath and A. J. Turberfield, *Nat. Commun.*, 2014, **5**, 5324.
21 A. J. Genot, D. Y. Zhang, J. Bath and A. J. Turberfield, *J. Am. Chem. Soc.*, 2011, **133**, 2177–2182.
22 B. Yurke and A. P. Mills, *Genet. Program. Evol. Mach.*, 2003, **4**, 111–122.
23 G. Seelig, D. Soloveichik, D. Y. Zhang and E. Winfree, *Science*, 2006, **314**, 1585–1588.
24 M. M. Maye, M. T. Kumara, D. Nykypanchuk, W. B. Sherman and O. Gang, *Nat. Nanotechnol.*, 2010, **5**, 116.
25 C. Zhang, R. Wu, Y. Li, Q. Zhang and J. Yang, *Langmuir*, 2017, **33**, 12285–12290.
26 Y. Zhang, A. McMullen, L.-L. Pontani, X. He, R. Sha, N. C. Seeman, J. Brujic and P. M. Chaikin, *Nat. Commun.*, 2017, **8**, 21.
27 R. P. Chen, D. Blackstock, Q. Sun and W. Chen, *Nat. Chem.*, 2018, **10**, 474–481.
28 F. Romano and F. Sciortino, *Phys. Rev. Lett.*, 2015, **114**, 078104.
29 S. H. Um, J. B. Lee, N. Park, S. Y. Kwon, C. C. Umbach and D. Luo, *Nat. Mater.*, 2006, **5**, 797.
30 N. Park, S. H. Um, H. Funabashi, J. Xu and D. Luo, *Nat. Mater.*, 2009, **8**, 432.
31 J. B. Lee, S. Peng, D. Yang, Y. H. Roh, H. Funabashi, N. Park, E. J. Rice, L. Chen, R. Long, M. Wu, *et al.*, *Nat. Nanotechnol.*, 2012, **7**, 816.
32 N. Conrad, T. Kennedy, D. K. Fygenson and O. A. Saleh, *Proc. Natl. Acad. Sci. U. S. A.*, 2019, **116**(15), 7238–7243.
33 L. Rovigatti, F. Bomboi and F. Sciortino, *J. Chem. Phys.*, 2014, **140**, 154903.
34 S. Biffi, R. Cerbino, G. Nava, F. Bomboi, F. Sciortino and T. Bellini, *Soft Matter*, 2015, **11**, 3132–3138.
35 D. T. Nguyen and O. A. Saleh, *Soft Matter*, 2017, **13**, 5421–5427.
36 W. H. Stockmayer, *J. Chem. Phys.*, 1943, **11**, 45–55.
37 P. J. Flory, *J. Am. Chem. Soc.*, 1941, **63**, 3083–3090.
38 J. S. Oh, Y. Wang, D. J. Pine and G.-R. Yi, *Chem. Mater.*, 2015, **27**, 8337–8344.
39 J. Fernandez-Castanon, S. Bianchi, F. Saglimbeni, R. Di Leonardo and F. Sciortino, *Soft Matter*, 2018, **14**, 6431–6438.
40 R. Pecora, *Dynamic light scattering: applications of photon correlation spectroscopy*, Springer Science & Business Media, 2013, pp. 1–384.
41 N. R. Markham and M. Zuker, *Nucleic Acids Res.*, 2005, **33**, W577–W581.
42 P. Šulc, T. E. Ouldridge, F. Romano, J. P. Doye and A. A. Louis, *Biophys. J.*, 2015, **108**, 1238–1247.
43 Z. Xing, A. Caciagli, T. Cao, I. Stoev, M. Zupkauskas, T. O'Neill, T. Wenzel, R. Lamboll, D. Liu and E. Eiser, *Proc. Natl. Acad. Sci. U. S. A.*, 2018, **115**, 8137–8142.